International Journal of Innovative Research and Scientific Studies, 8(5) 2025, pages: 1360-1375

IJIRSS
International Journal of Innovative Research & Scientific Studies

ISSN: 2617-6548

URL: www.ijirss.com

Design, simulation, and analysis of a solar-powered street lighting control system for power consumption prediction

Junisbekov M. Sh[1], Dmitriy Grigoryev[2*], Turgynbekov Ye[2], Zhanar Omirbekova[2]

[1]*Taraz University named after M.Kh.Dulaty,Republic of Kazakhstan.*
[2]*Kazakh National Research Technical University named after K. Satbayev,Almaty 050013, Republic of Kazakhstan.*

Corresponding author: Dmitriy Grigoryev (*Email: dgrigd@mail.ru*)

Abstract

This paper presents a digital model of an intelligent solar-powered street lighting system with integrated energy consumption forecasting, developed in MATLAB/Simulink. The simulation uses real hourly weather data from the Almaty region, where solar irradiance ranged from 0 to 980 W/m² and temperatures varied from –25°C to +35°C. The modeled system includes a 200 W photovoltaic panel, a 120 Ah battery, and LED luminaires up to 60 W. Predictive analysis of the battery's state of charge (SOC) and need for external power was conducted using AI algorithms ANN, LSTM, GRU, and Random Forest trained on synthetic data from the simulation. Results show the system can operate autonomously for up to 72 hours under adverse weather. The probability of switching to backup power is 27–32% in winter and under 8% in summer. The LSTM and GRU models achieved a mean SOC prediction error of less than 5% versus actual values. The proposed architecture offers a practical and adaptable approach for designing, testing, and optimizing solar-powered lighting in both urban and rural settings across Kazakhstan and similar regions. It demonstrates the potential of combining simulation with AI to support sustainable and resilient outdoor lighting infrastructure.

Keywords: Artificial neural networks, Energy efficiency, Energy management, LED lighting, MATLAB Simulink, Smart lighting, SOC prediction, Solar energy prediction, Solar system simulation.

DOI: 10.53894/ijirss.v8i5.9136
Funding: This work is supported by the Science Committee of the Ministry of Science and Higher Education of the Republic of Kazakhstan, Kazakhstan (Grant number: AP19679604).
History Received: 16 June 2025 / **Revised:** 18 July 2025 / **Accepted:** 22 July 2025 / **Published:** 6 August 2025

Competing Interests: The authors declare that they have no competing interests.
Authors' Contributions: All authors contributed equally to the conception and design of the study. All authors have read and agreed to the published version of the manuscript.
Transparency: The authors confirm that the manuscript is an honest, accurate, and transparent account of the study; that no vital features of the study have been omitted; and that any discrepancies from the study as planned have been explained. This study followed all ethical practices during writing.
Publisher: Innovative Research Publishing

1. Introduction

Public street lighting systems constitute a significant portion of urban energy consumption, making them prime targets for energy efficiency improvements. As urbanization progresses and living standards increase, the demand for reliable power expands not only in densely populated cities but also in remote rural areas where lighting is essential whenever human presence is expected. In this context, solar-powered lighting systems present a sustainable and increasingly viable alternative. Photovoltaic (PV) panels tend to have a long operational lifespan, typically between 20 and 35 years, with ongoing improvements in energy conversion efficiency. These features make solar-powered systems an attractive solution for modern, energy-conscious infrastructure. However, solar lighting systems face several challenges, particularly those related to weather variability and the intermittent nature of solar energy. As noted in United Nations Economic Commission for Europe [1] renewable energy sources require advanced digital technologies to maintain grid stability due to their unpredictability. This study introduces a simulation model designed to evaluate key parameters of solar-powered street lighting systems. It supports the integration of artificial neural networks (ANNs) to predict the system’s battery state of charge (SOC) and to estimate critical discharge moments. While multiple AI models have been proposed for SOC prediction using weather data, this research distinguishes itself by providing a simulation framework that can generate training data even when real-world measurements are unavailable common during early design phases or when adapting systems to new locations. The primary goal of this paper is to enable precise prediction of a smart lighting system’s power demand. For this purpose, a simulation-based imitation model has been developed. Given forecasted weather conditions, the model predicts when the internal battery will be depleted and when supplementary energy from an external source will be necessary. The proposed model is notable for its transparency, as all operational parameters are fully measurable and observable during system operation. Its flexibility allows for easy adaptation to various system configurations and constraints, while its universality ensures it can be applied to a wide range of energy prediction tasks. The research focuses on creating a universal mathematical simulation model, simulating smart lighting systems with both synthetic and real-world weather data, developing and training AI models on simulated datasets, and conducting comprehensive analyses to compare results across different input sources.

Lighting public areas and streets significantly contributes to electrical consumption. With increasing interest in power-efficient technologies, numerous efforts have been undertaken in this field, resulting in a substantial body of literature on the topic. Generally, leading authors present several common ideas. First, they recommend replacing different types of lamps with more energy-efficient LEDs. Many publications demonstrate the benefits of such replacements and brief payback periods [2]. The https://www.zgsm-china.com/blog/how-much-do-the-street-lights-cost.html estimates a payback period of 2.1 years for LEDs and 2.85 years for solar-powered lamps. In conclusion, it is strongly advised that all lighting be replaced with LEDs, and the resulting savings be calculated. Others suggest implementing sophisticated control algorithms for the lamps [3, 4]. In this case, savings are achieved by reducing the power consumption of each unit, often by decreasing the active hours or brightness [4] under certain conditions. Typically, this reduction correlates with the presence of people or vehicles in the lit area. Some articles assess the existing object and base decisions on its recognition whether it is an animal or a human. Advanced algorithms are employed to identify objects and their speed through simple camera systems [5]. Another significant group of authors advocates using alternative power sources for street lighting, such as solar PV panels or wind turbines [6]. These systems are usually designed to be entirely independent of other power sources [6, 7] which can pose issues in severe weather conditions over extended periods. Without backup power, all batteries risk discharging simultaneously, potentially plunging regions into darkness a dangerous scenario. Our scope is to predict this moment in terms of time [7] or remaining power capacity to decrease the negative consequences. Many researchers report measured data from devices and installations recorded over specific periods [7, 8]. In Ożadowicz and Grela [3] the authors utilize standard industrial measurement solutions available on the market, which can be advantageous for replication, standardization, and certification. However, for large-scale deployment, this approach is often more costly than custom-designed systems built from affordable components. Researchers also frequently employ various modelling tools such as MATLAB and Simulink [6, 9]. In Li et al. [10] PV power prediction is based solely on historical data, with analysis distinguishing between inter-day and intra-day parameters. A recurrent neural network (RNN) is trained to forecast PV power within 15 to 90 minutes using only historical data, yielding promising results compared to other methods. In Dewangan et al. [11] different modelling architectures are compared for forecast accuracy, using a universal model for all lead times and separate models for each hour of the following day. The impact of retraining frequency on prediction accuracy is also examined. Efforts to improve weather prediction quality include adapting neural network structures and hyperparameters for greater accuracy. For example, in Chai et al. [12] the LSTM network is enhanced with time-weighted coefficients and an improved activation function, along with methods like Momentum Resistance Weight Estimation and adaptive learning factors. As a result, the AHPA-LSTM model is proposed with improved capabilities. Despite these advances, the modeling and simulation of solar lighting systems are relatively underrepresented in specialized literature. In Valiullin [9] a distribution network simulation model based on matrix iteration is detailed, employing a point-based method to calculate light intensity. Control strategies include timetable-based switching and real-time intensity control, which incorporate traffic flow as a key influencing factor. Validation was achieved through actual measurements. In Nymann et al. [13] researchers built a spatial laboratory to measure voltage-current characteristics of solar-powered lighting, developing a MATLAB-based simulation tool and a control device for managing LED lamps and batteries. They successfully demonstrated the system's predictive capabilities in real-world applications. After deploying any project, it is essential to assess its impact and gather feedback from the public. In Akindipe et al. [14] a comprehensive framework for such evaluation is proposed, considering costs, savings, environmental benefits, maintenance, and social factors. The study includes stakeholder surveys revealing a preference for hybrid solar-grid solutions (62%). Notably, few publications explore lighting system simulations from a meteorological perspective or investigate the relationship between weather parameters, system behavior, and AI-based predictions. This research aims to evaluate the accuracy and reliability of power generation forecasts within a simulation framework, encouraging further investigation in this area. It is the first in a series exploring this topic, with future work planned to optimize device design and physical implementation.

The primary objective of this study is to develop, simulate, and analyze an intelligent solar-powered street lighting system with energy consumption forecasting capabilities, tailored to the climatic and operational conditions of Kazakhstan. The research aims to construct a universal digital imitation model within the MATLAB/Simulink environment, enabling evaluation of the performance of a hybrid configuration comprising a solar panel, battery storage, LED luminaires, and a backup power source under various weather and usage scenarios. Additionally, the study implements artificial intelligence methods to predict critical operating states and automate energy consumption management.

2. Methods

2.1. Mathematical Model

To accurately analyze the performance of the solar-powered street lighting system and enable the training of predictive AI models, a comprehensive mathematical description of all major components and energy flows is developed. The key system elements include a photovoltaic (PV) panel, a rechargeable battery, a sensor-controlled LED load, and a control subsystem.

2.1.1. Energy Balance Equation

The following equation describes the overall energy balance over a 24-hour period:

$$E\_total = E\_PV + E\_ext + E\_loss - E\_LED \tag{1}$$

where: E_PV — Energy generated by the PV panel (Wh), E_ext Energy supplied by an external power source (Wh), E_loss —System losses, including power electronics, cabling, and battery inefficiency (Wh), E_LED Energy consumed by the LED lighting load (Wh)

The control system is configured such that when the battery state of charge (SOC) drops below a critical threshold (e.g., 15%), the system switches to an external power supply to ensure reliable lighting.

2.2. Photovoltaic Panel Model

The power output of the PV panel at a given time is calculated as:

$$P\_PV(t) = \eta\_PV * A\_PV * G(t) * [1 - \beta(T\_cell(t) - T\_ref)] \tag{2}$$

where: η_PV — Nominal efficiency of the PV panel, A_PV — Surface area of the PV panel (m²), G(t) — Solar irradiance at time t (W/m²), β — Temperature coefficient of efficiency (typically 0.3–0.5%/°C), $T\_cell(t)$ — PV cell temperature at time t (°C), T_ref — Reference temperature (25°C).

$$\mathrm{E\_PV} = \int_0^{24} P\_PV(t)dt \tag{3}$$

2.3. Battery Model

The battery is modelled as a second-order RC equivalent circuit with a thermal model and SOC output. The SOC at time t is updated as:

$$SOC(t+1) = SOC(t) + [\eta\_c * I\_ch(t) - I\_dis(t) / \eta\_\mathrm{d}] / \mathrm{C\_bat} * \Delta \mathrm{t} \tag{4}$$

where: SOC(t) — Battery state of charge at time t (0–1 or 0–100%), $I\_ch(t)$ — Charging current (A), $I\_dis(t)$ — Discharging current (A), η_c — Battery charge efficiency, η_d — Battery discharge efficiency, $\mathrm{C\_bat}$ — Rated battery capacity (Ah), Δt — Time step (h)

$$\mathrm{C\_bat(T) = C\_bat, ref} * [1 + \alpha(\mathrm{T - T\_ref})] \tag{5}$$

where α is the temperature coefficient for capacity.

2.4. LED Load and Presence Sensor Model

The LED load is operated in two main modes:

- Full brightness (P_LED,100): during peak activity hours and upon presence detection.
- Reduced brightness (P_LED,33): during night mode, when no presence is detected.

$$\mathrm{P\_LED(t) = S\_pres(t) * P\_LED.100 + [1 - S\_pres(t)] * P\_LED.33} \tag{6}$$

$$E\_LED = \int_0^{24} P\_LED(t)dt \tag{7}$$

2.5. Losses

System losses include:

- Power electronics and controller consumption P_ctrl
- Battery self-discharge and leakage P_leak
- Thermal losses in cables and conversion

$$E\_loss = \int_0^{24} [P\_ctrl(t) + P\_leak(t)]dt \quad (8)$$

2.6. Summary System Flow

The complete simulation iteratively updates SOC, battery temperature, and LED operation at each timestep, based on input irradiance and presence sensor signals, providing a detailed profile of system performance for any location or scenario.

The above mathematical model serves as the basis for both the simulation in MATLAB/Simulink and the training of AI predictive models (such as ANN, LSTM, and GRU) using real or synthetic weather and presence data. Model parameters can be adapted to specific local conditions, equipment types, and user-defined operational strategies.

3. Research Hypothesis

The central hypothesis of this research is that integrating digital simulation in the MATLAB/Simulink environment with artificial intelligence techniques including neural networks such as LSTM and GRU can significantly enhance the accuracy of predicting critical battery operating states and optimize energy management in autonomous solar-powered street lighting systems. The developed model is expected to support autonomous lamp operation for at least 70 hours, even under unfavorable weather conditions, with an average prediction error for battery state of charge (SOC) not exceeding 5% compared to actual measurements.

3.1. Scientific Novelty

- For the first time, an adaptive digital model of a solar-powered street lighting system tailored to Kazakhstan's climatic conditions has been developed in MATLAB/Simulink, featuring integration capabilities with AI-based forecasting algorithms.
- A universal modeling approach has been formulated, enabling the use of both real meteorological data and synthetically generated or online-imported weather series for simulation, significantly broadening the model's applicability and testing potential.
- The system architecture incorporates automated prediction of battery threshold states and dynamic operational mode switching using advanced neural network techniques (ANN, LSTM, GRU) and ensemble algorithms.
- A systematic evaluation of different AI models has been conducted on both synthetic and real-world datasets, allowing for the identification of the most effective solutions in terms of energy reliability and system resilience.
- The obtained results confirm the potential of digital twins and intelligent algorithms for accelerating deployment, optimizing performance, and customizing autonomous lighting systems for diverse climatic conditions across regions.

3.2. The logic of the LED Lamp Operation is the Following

The lamp's battery charges during daytime. The duration of this phase depends on the season and geographical location. Then, when the Sun is down, the LED is 100% on from sunset until 24:00. Starting from 00:00, the LED enters night mode. This means that it is switched on only 33% of its brightness if no presence is detected and 100% if a presence signal arrives. This signal could originate from its PIR detector (or another type of sensor), one of the nearest lamp pole's systems, or a supervisory system. If no new presence signal arrives, the LED remains at maximum power for a period such as 5 minutes and then reverts to 33% brightness. This operational mode remains active until 06:00. From 06:00 until sunrise, the LED is on at 100%. During the day, the system is in charging mode.

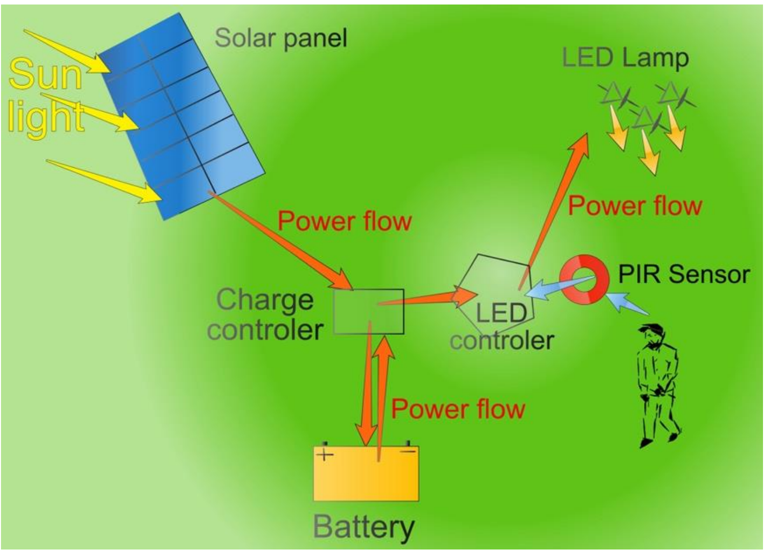

Figure 1.
Model power flow.

Figure 1 illustrates the operating principle of an autonomous solar-powered street lighting system equipped with a passive infrared (PIR) motion sensor. The photovoltaic panel converts solar radiation into electrical energy, which is transferred via a charge controller to the battery for storage. Upon motion detection by the PIR sensor, the LED lamp is activated and powered through an LED driver connected to the battery. Red arrows indicate the direction of energy flow between system components. This configuration ensures automatic and energy-efficient nighttime illumination.

The external power source is used when the battery's SOC drops below a certain level, for example, 15%. The external power supplies LEDs at night.

Power balance for 24 hours of operation:

$$W_{SUN} + W_{EXT} = W_L + W_{LED} \quad (9)$$

In Equation 1: W_{SUN} is the panel-generated energy, W_{EXT}- energy from an external power source, W_L – losses, including control system and communication consumption, W_{LED} – power to the LED light.

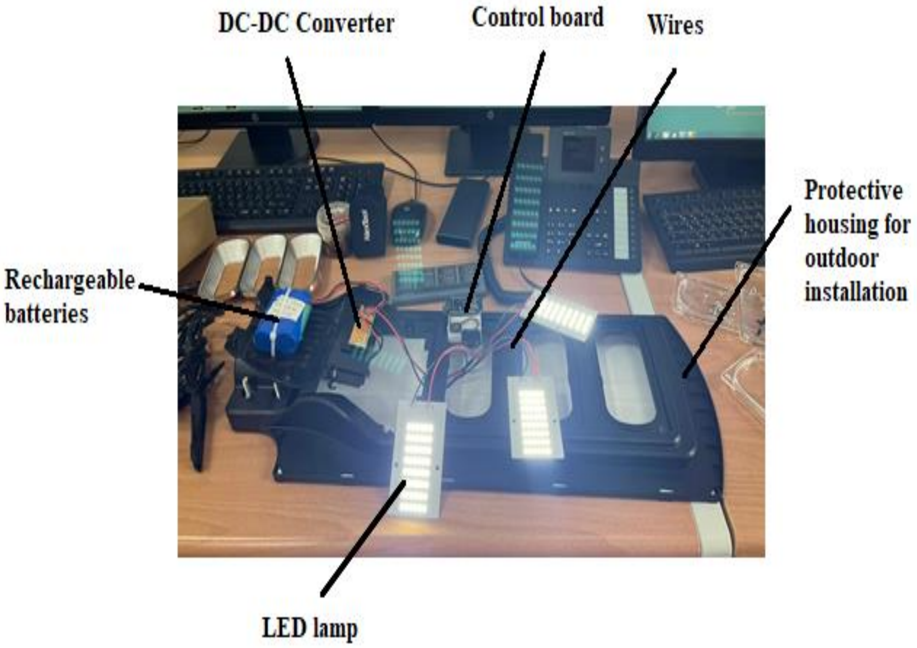

Figure 2.
Hardware configuration of the autonomous solar-powered street lighting system with a PIR motion sensor.

Figure 2 shows the hardware setup consisting of a control board, battery units, three LED modules, interconnecting wiring, and a protective enclosure designed for outdoor installation. This configuration is used to verify the power supply scheme, battery charging from the solar panel, and the operation of the LED lamps based on signals from the motion sensor. The assembly is tested on a laboratory bench prior to its final deployment outdoors, thereby confirming the practical implementation of the system illustrated in the schematic.

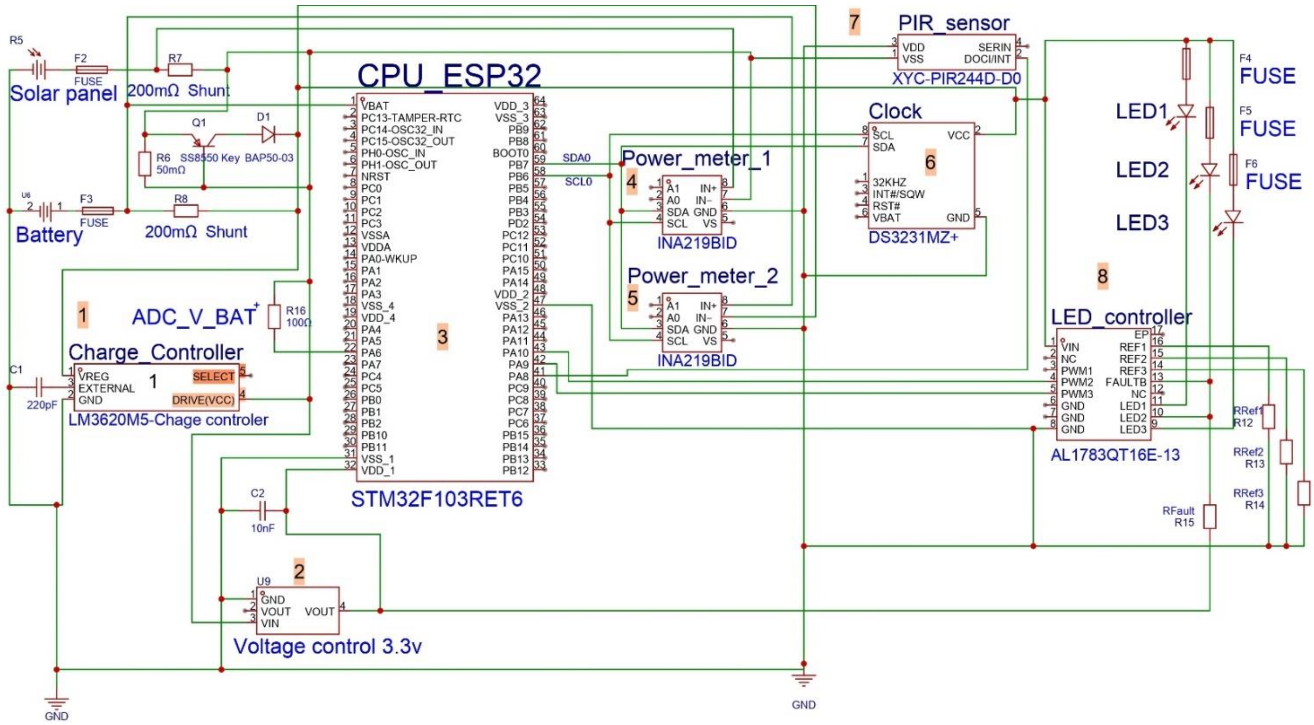

Figure 3.
Structural layout of the lamp housing with an AD31 aluminum alloy solar panel.

The figure presents a schematic of a lamp housing made from anodized AD31 aluminum alloy, designed for integration with a solar panel. The system is controlled by an STM32F103RET6 microcontroller (1) and powered by a rechargeable battery (2), charged via a 5 V solar panel (3) protected by fuses (4). The LM3620M5 charge controller (5) ensures stable charging and battery protection, while voltage regulation at 3.3 V is maintained by the U9 regulator (6). Two INA219BID modules (7) measure currents up to 3.2 A and voltages up to 26 V in both the battery and load circuits for precise energy monitoring. The DS3231MZ+ real-time clock module (8) maintains accurate timing with an error margin under 2 ppm. A PIR sensor (9) detects motion within a 6 m range. LED indicators (10) are driven by an AL1783QT16E-13 driver (11), capable of handling up to 150 mA per channel, enabling efficient status indication and system signaling.

Figure 4.
Solar street lamp with a housing made of AD31 aluminum alloy.

Figure 4 presents a solar-powered street lamp featuring a housing constructed from anodized AD31 aluminum alloy. This material offers high corrosion resistance, lightweight structural properties, and long-term durability under outdoor operating conditions. The anodized surface provides additional protection against environmental exposure and mechanical damage, significantly extending the service life of the device while preserving its aesthetic appearance over prolonged periods of use.

The following software tools used in this research include MATLAB 2016a, with Simulink version 8.7, employed for simulation modeling. For artificial intelligence (AI) training and verification, Python 3.10 was utilized, along with the libraries Keras 3.6, NumPy 1.26.4, Pandas 2.2.3, and TensorFlow 2.18.0. The Python environment was operated on Ubuntu 22.04.5 on a Vector GP 68 HX laptop. Neural network training was accelerated using a GPU.

4. Simulation Method

The methodology employed involves the simulation of actual system behavior using Simulink. In the first set of experiments, solar power is represented by a sinusoidal waveform with random components added to mimic realistic fluctuations. Using different periods, the model simulates fluctuations in weather conditions, such as shifts from cloudy to sunny intervals. A primary sinusoidal function emulates daily changes in daylight, enabling the model to replicate the climate dynamics of any specific region. The photovoltaic (PV) panel's voltage and generated power values are obtained as outputs.

The second simulation method involves using solar power input, leveraging online data services. For enhanced realism, actual meteorological data from a weather station and satellite data are also incorporated into the simulation [15]. Additionally, forecasted weather data can be utilized to refine simulation accuracy further.

The third method incorporates actual solar power intensity measurements obtained from a local weather station in the Almaty region. The use of real-world data yielded results closely matching those from synthetic data.

Simulated in the Simulink tool, the street lighting model output values were extracted from MAT files, processed, and utilized for AI predictive model training and validation in Python. The performance of the AI models was then evaluated using standard metrics and compared.

4.1. The Imitation Model Input Data Visualization and Comparison

The simulated solar intensity data generated through sinusoidal functions provides results that align well with real-world observations. For instance, simulated values closely follow the patterns of the values from the İkitelli Solar Power Plant [16]. Figure 2 illustrates actual data obtained from the İBB Open Data Platform, recorded in August 2018. This dataset comprises 15-minute interval measurements from a 1200 kW solar power plant in the Istanbul Water and Sewerage Administration (ISKI) Ikitelli Drinking Water Treatment Plant. The data spans from May 2018 to May 2019 and confirms the model's efficacy in reproducing realistic solar power generation patterns based on weather simulations.

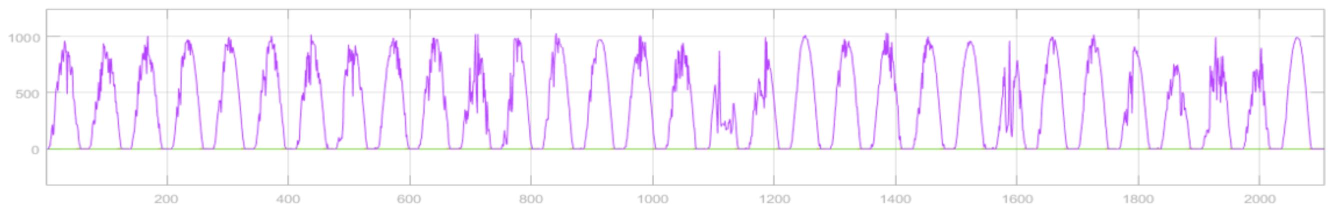

Figure 5.
Sun power values from the solar power station in Turkey in August 2018 measured in 15-minute steps.

Figure 5 presented of a similar patterns observed in data from online sources such as the Photovoltaic Geographical Information System (PVGIS) [16] which provides solar power intensity data for various global locations. PVGIS offers time series data on solar radiation and photovoltaic (PV) performance, available hourly, daily, or monthly for selected regions. Historical data ranges from 2005 to 2023, with available values for solar radiation, estimated PV system performance, and other metrics. This data, derived from satellite measurements and, in some cases, reanalysis, enables extensive solar power simulation and analysis.

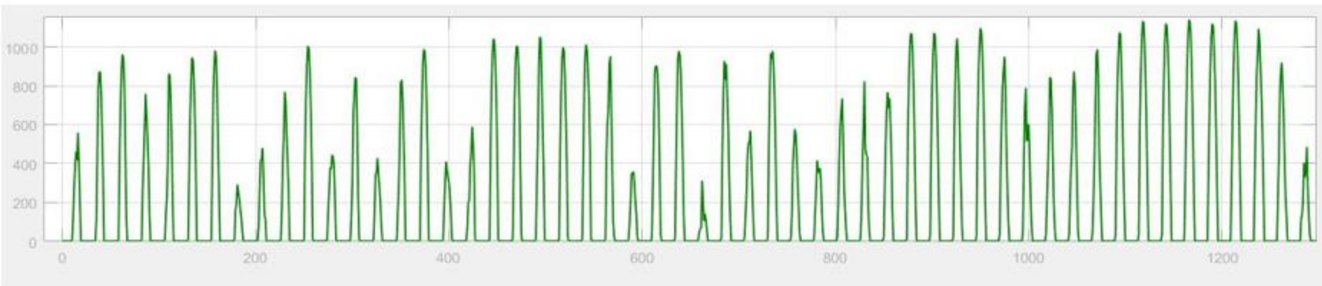

Figure 6.
A sample dataset from PVGIS for the Almaty region, showing hourly values over 54 days.

Figure 6 presents a sample dataset from PVGIS for the Almaty region, showing hourly values over 54 days in 2005, the initial period from the available dataset. The resulting data demonstrates a sinusoid-like pattern in shape and distribution, reinforcing the similarity between PVGIS-derived values and an approximating sinusoidal pattern.

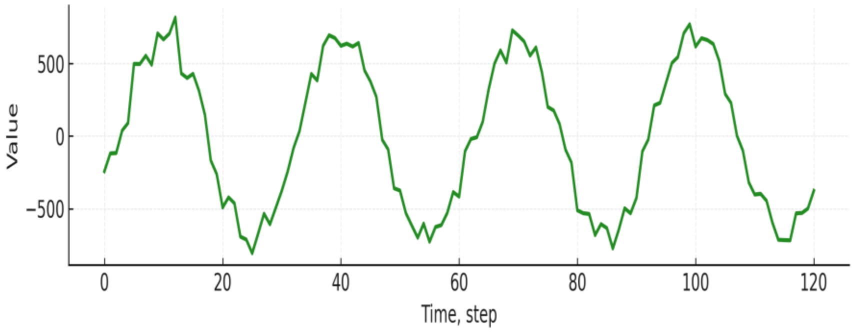

Figure 7.
Variation of the studied parameter (e.g., power or current) over time with a unit step.

Figure 7 illustrates the variation of a studied parameter, such as power or current, over time with a step size of one. The plot exhibits distinct cyclical fluctuations: values rise periodically to 600–700 and drop to –500 to –600 in a repeating pattern. This behavior reflects day–night transitions or alternating operational and idle cycles typical of processes influenced by renewable energy sources and weather dynamics.

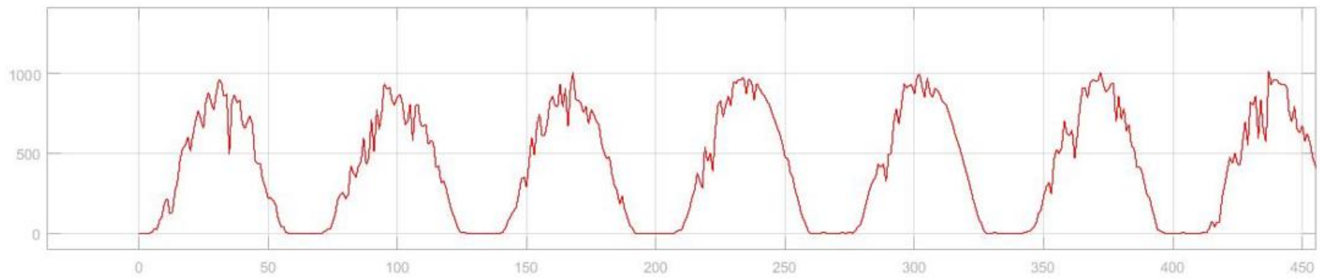

Figure 8.
Hourly irradiance values from the Photovoltaic Geographical Information System (PVGIS) for the Almaty region.

Figure 8 displays irradiance values obtained from the Photovoltaic Geographical Information System (PVGIS) for the Almaty region, presented in one-hour intervals. The chart shows pronounced diurnal fluctuations in solar radiation, with peak values reaching 900–1000 W/m² during daylight hours and dropping to near zero at night. These data confirm the presence of a stable, repetitive cycle in solar intensity, an essential factor for accurate modeling and analysis of solar energy systems in the specified region.

4.2. Weather Simulation

Weather simulation involves varying climatic conditions to test the lighting system's performance. This includes daylight intensity, cloud cover, and temperature. Actual weather data from local stations and synthetic data are used to validate the model. Input data can be either actual or predicted values. If predicted values are used, it is possible to forecast future photovoltaic (PV) generation with reasonable accuracy.

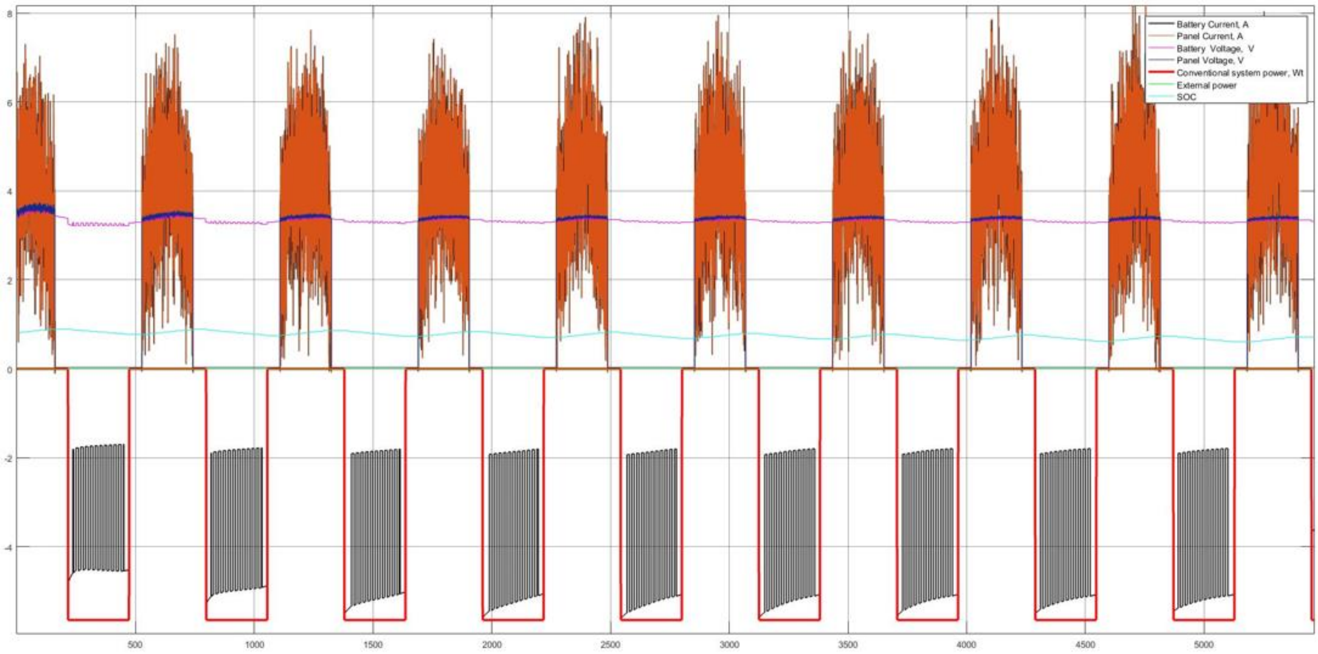

Figure 9.
Data output from the simulation model in Simulink.

Figure 9. Operating parameters of the solar-powered system over 1800 simulation time steps.

Figure 9 illustrates the operating parameters of the solar energy system over a time span of 1800 simulation steps. The orange curve ("PV panel output") represents the photovoltaic panel's power output, with daytime peaks reaching approximately 800–900 W. Variations in output are attributable to weather conditions, while values drop near zero at night and during overcast intervals. The blue line ("Power") indicates that during battery charging phases, power increases linearly up to 500 W, and during discharging, it decreases to –500 W or lower. The light-blue line ("Battery voltage") reflects a gradual decrease in battery voltage from 1200 V at the beginning of the cycle to about 1050 V at the end. The graph clearly demonstrates the battery's charge-discharge cycles and the dependence of solar power output on the time of day.

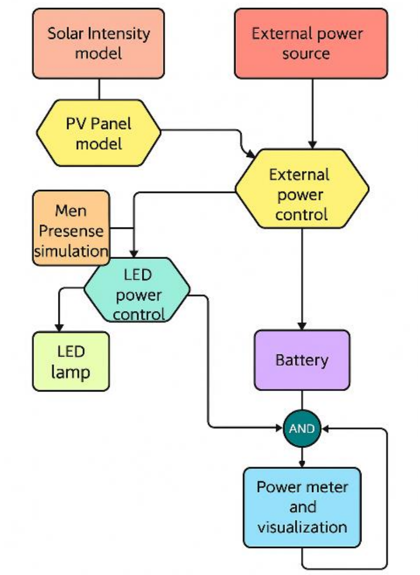

Figure 10.
Simulink Model data flow.

Figure 10. Data flow and interaction between core components of the solar lighting simulation model.

Figure 10 illustrates the data flow and interconnection of key components within the simulation model of the solar-powered lighting system. The diagram includes modules for solar irradiance simulation, battery charging, LED lamp power control, and the external power supply unit. The system accounts for both the energy supplied by the photovoltaic panel and the fallback to external power when the battery charge is insufficient. All component outputs are routed to a visualization module, enabling real-time monitoring of system status. The diagram provides a comprehensive view of the hybrid lighting system's operational logic under various working scenarios. At night, the presence of objects such as cars or people within the lamppost area is simulated using a periodic pulse source. Each pulse represents an instance of object presence, activating full power of the LED. A constant pulse generator with a 50% pulse width simulates object presence near the pole during nighttime. This generator is active throughout the night hours, representing nighttime activity around the pole or external signals to increase brightness. This includes emergency signals from a control center or nearby poles detecting cars or pedestrians.

This model is a part of the Simulink Simscape library - the second-order RC circuit with thermal model and the state of charge (SOC) output value.

Parameters of the battery model are presented as tables with the R and C values. These values vary for different battery models, vendors, conditions, etc. The thermal model consists of an ideal heat flow source and the battery's thermal mass.

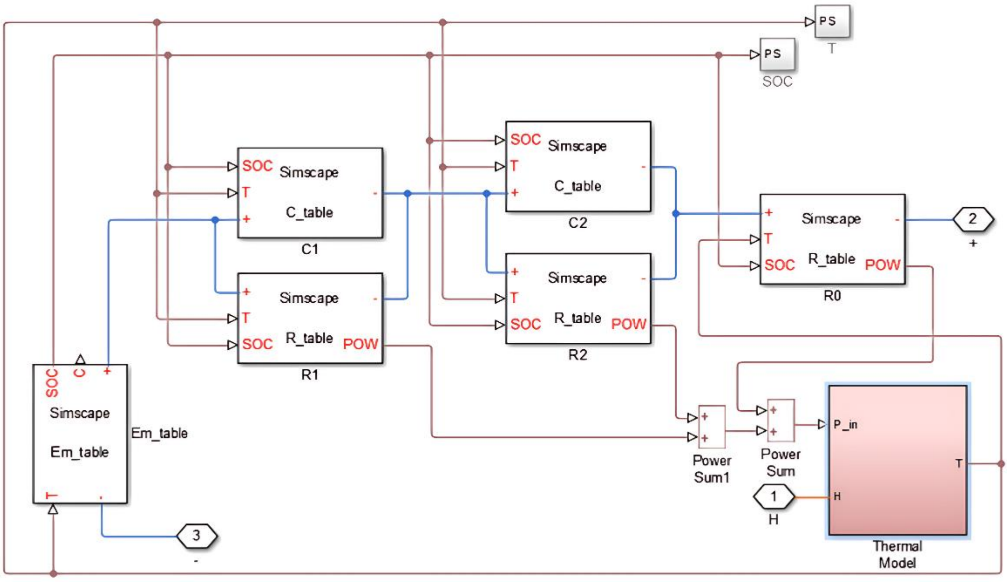

Figure 11.
Battery model with integrated thermal analysis implemented in Simulink/Simscape.

Figure 11 presents a battery model incorporating thermal dynamics, developed within the Simulink/Simscape environment. The system includes multiple components: blocks C1, C2, R1, R2, and R0 simulate the capacitive and resistive characteristics of different battery sections. Input data such as energy, temperature, and state of charge (SOC) are fed into these blocks, enabling detailed calculations of power distribution, thermal losses, and battery condition over time. The computed outputs are forwarded to a thermal model module, which determines the aggregate temperature and thermal behavior of the battery during operation. This modeling structure enables a comprehensive analysis of electrochemical and thermal processes in battery systems under diverse operating conditions.

5. Results and Discussion

The system's core synchronization relies on a sinusoidal signal representing the daily solar intensity cycle. This sine wave coordinates the charge-discharge cycles, presence sensor signals, and LED control logic. It has a period of 24 hours in relative time units. Additional sinusoidal waves with shorter periods and random multipliers are used to simulate variable weather conditions like clouds, smog, etc., while long-period sine waves model annual variations of solar intensity, ideal for year-long simulations. Band-limited white noise further randomizes weather conditions, enhancing the simulation's realism. Power and average of the solar intensity value depend on geographical location and correspond to real local climate conditions.

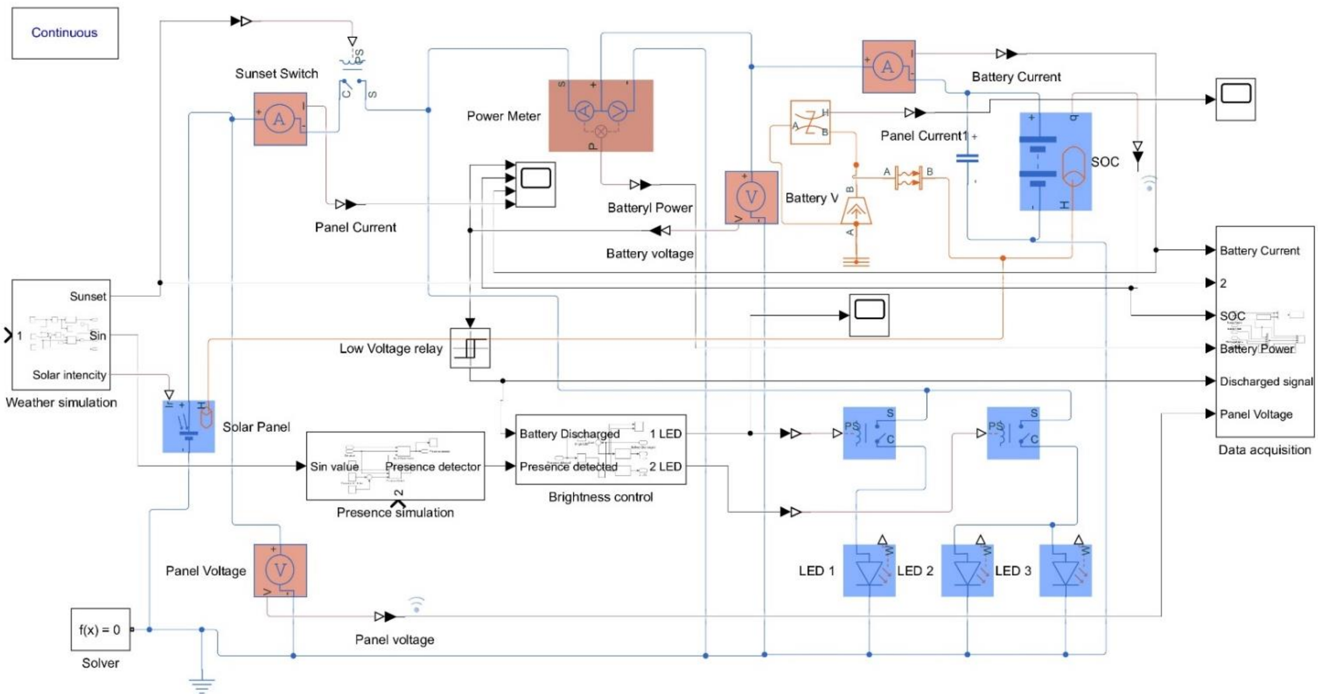

Subsystem for the weather simulation (A)

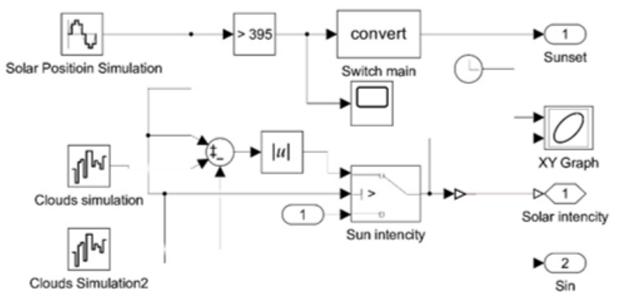

Subsystem for presence simulation (B)

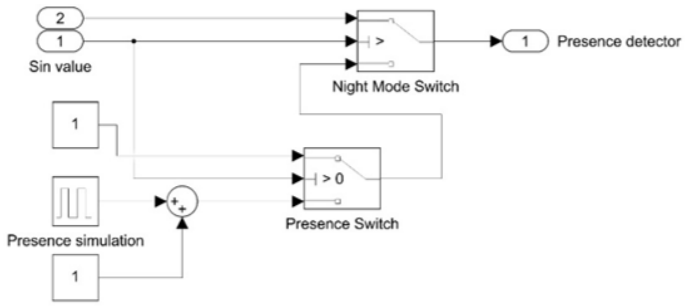

Subsystem for the LED brightness control (C)

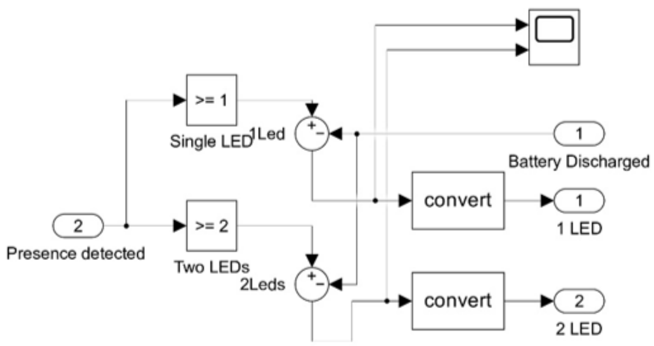

Subsystem for the data acquisition (D)

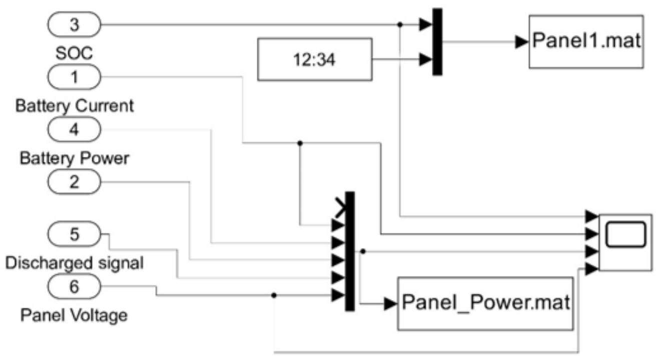

Figure 12.
Lighting system imitational model in Simulink.

Figure 12 shows a comprehensive model of the energy and control system implemented in MATLAB/Simulink. The core logic for energy flow control between the battery, solar panels, load, and power sources is placed centrally in the scheme. Numerous measurement units, control blocks, and signal lines (highlighted in blue and black) are used, enabling simulation of hybrid system operation under various scenarios. This model facilitates simulation, analysis, and optimization of energy system performance, considering real-world factors from charge dynamics to external influences and source-switching logic.

A basic model of a conventional LED lighting system with constant-brightness LEDs used as a reference to compare and evaluate the energy efficiency of smart lighting.

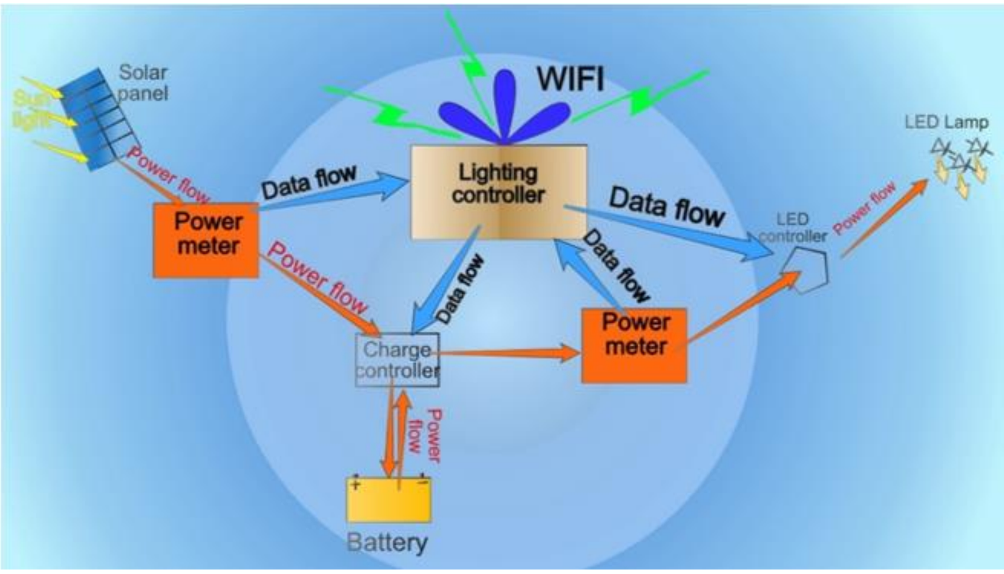

Figure 13.
Data transmission in the lamp control system.

Figure 13 illustrates the structural diagram of the intelligent solar lighting system with remote control via WiFi. The solar panel converts solar energy into electricity, which flows through a power meter and charge controller into the battery. System status and power flow data are collected and transmitted via the 'data flow' channel to the central lighting controller, which monitors and controls LED lamp operation. The controller supports remote data exchange via WiFi and manages the load via the LED controller, optimizing power consumption based on sensor feedback. The diagram effectively demonstrates the integration of IoT components, energy monitoring, and intelligent control in an autonomous street lighting system.

During the Simulink simulations, an overvoltage phenomenon was observed during the PV power supply connection and disconnection. In these instances, the PV voltage spikes significantly, reaching up to ten times its nominal value. This effect will be further investigated and documented in future studies. A protective feedback signal from the power sensor was incorporated to mitigate this overvoltage, disconnecting the power supply when overvoltage is detected. This protection mechanism can be implemented in real systems for enhanced safety.

Power, current, and voltage are measured using standard Simulink meters from the library, and the values are saved to an output MAT file, containing time values, solar intensity, and power consumption. Using Python, this data is extracted into a CSV file for further processing, including normalization, preparation, and splitting.

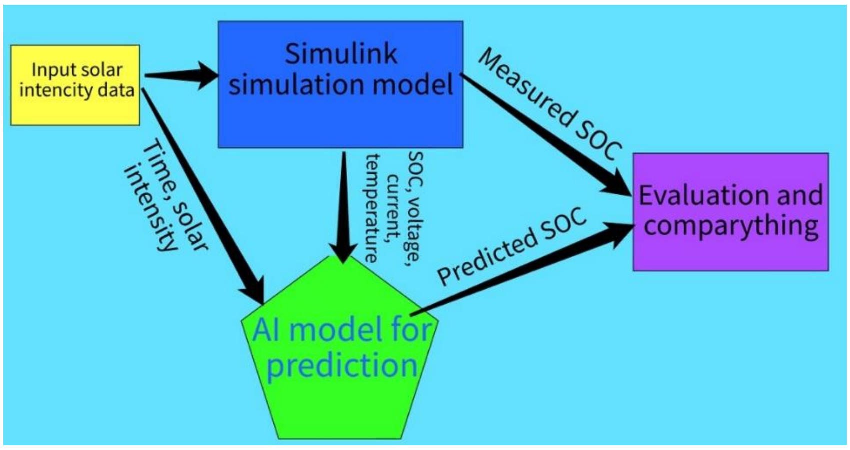

Figure 14.
Imitational and AI models data flow.

Figure 14 presents the interaction structure between models for predicting the battery's state of charge (SOC) using artificial intelligence. Simulink receives solar irradiance as input, after which system parameters such as voltage, current, and temperature are formed. These are fed into the AI model, which predicts SOC. The predicted values are then compared with measured SOC data, and the results are analyzed to evaluate model accuracy. This approach enables the validation and improvement of AI algorithms using simulation data.

5.1. The Following Experiments Implemented

1. Synthetic random values are used as sunlight intensity input for the solar panel simulation model in Simulink to model power generation. Both generated and consumed power are measured and utilized for training the machine learning

(ML) model. The presence sensor signal is simulated at a preset frequency. The load can be considered constant at this stage but may vary in real life due to seasonal changes, weekends, and other factors.

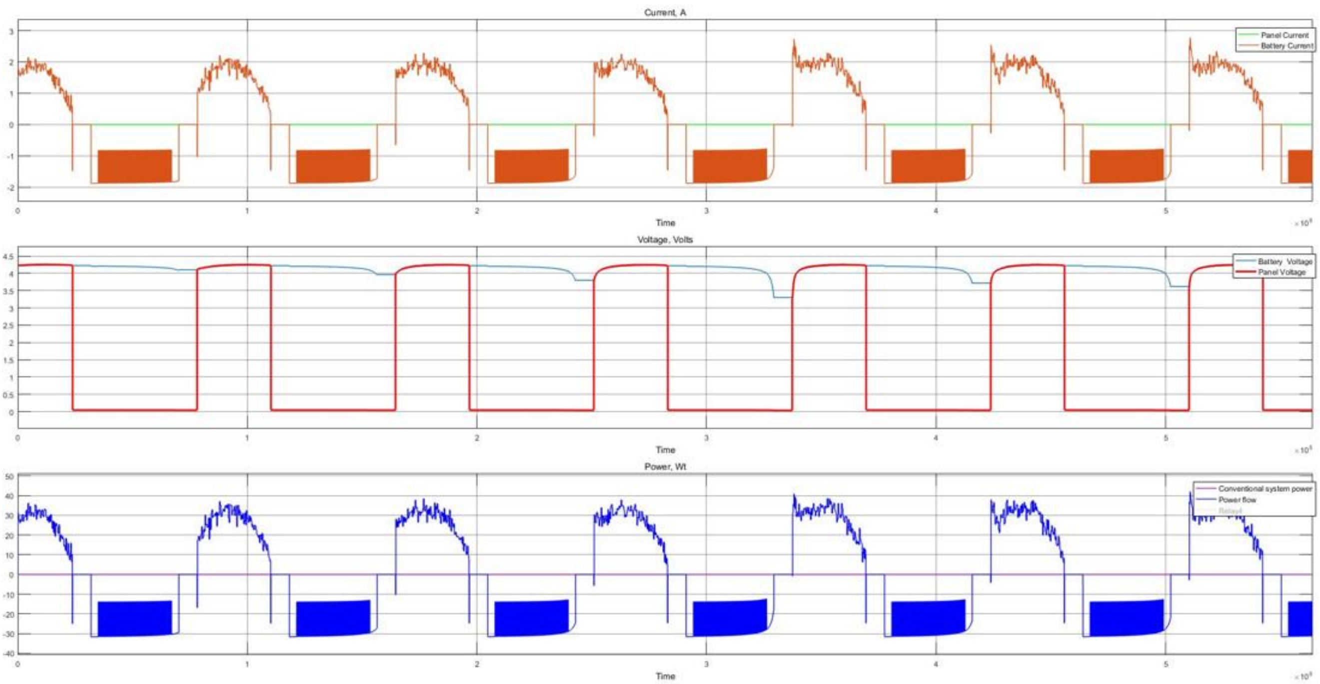

Figure 15.
Simulink solar-powered lamp model output with random simulated solar intensity for 11 days.

Figure 15 shows the daily operational cycles of a hybrid solar energy system over 6000 simulation steps. The orange line ('PV panel current') indicates solar panel current output: during daylight, it peaks at 1400–1500 mA, dropping to zero at night and under cloudy conditions. Black triangles ('Battery current') illustrate battery charging and discharging: charging peaks at +1000 mA during the day, while discharging reaches –900 mA at night. Panel and battery voltages (purple and yellow lines) remain nearly constant around 4.1–4.2 V. The red line ('Conventional system power consumption') lies along the X-axis, indicating negligible external load during the period.

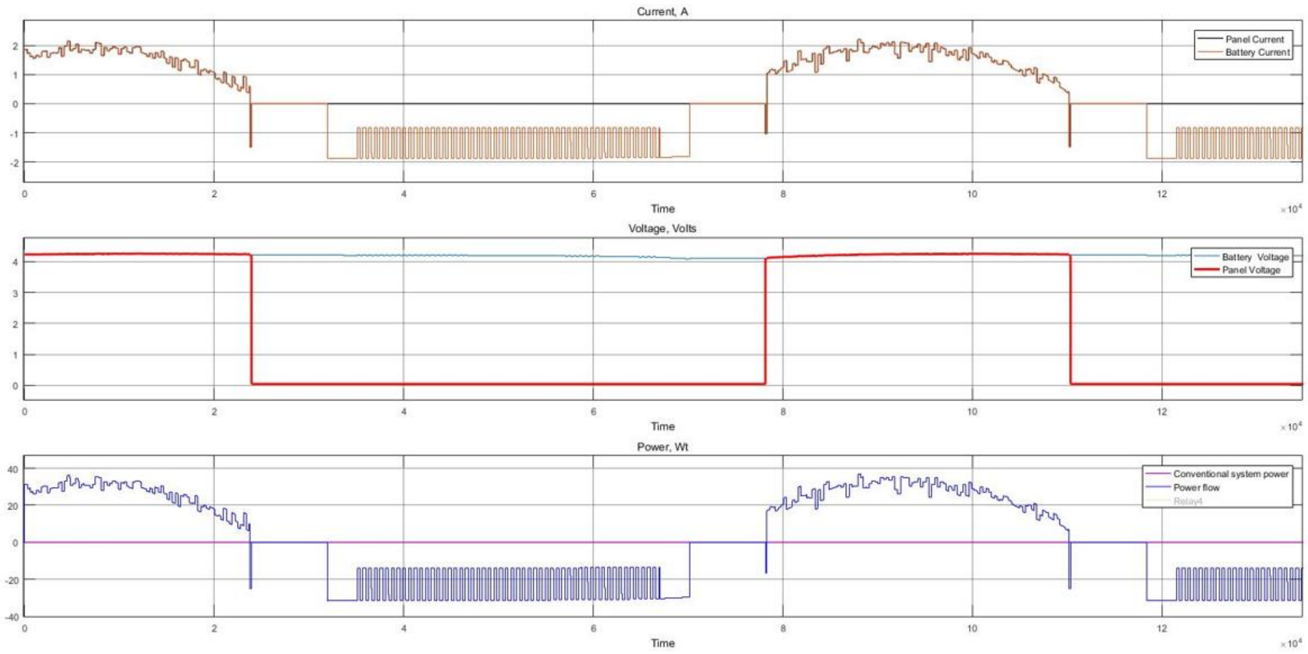

Figure 16.
Simulink solar-powered lamp model output with simulated solar intensity for 1 day.

Figure 16 presents operational parameters of the hybrid energy system between 1100 and 1900 simulation steps. The red line ('Conventional system power consumption') indicates three main load activity periods: approximately 1200–1330, 1420–1510, and 1850–1900. During these intervals, battery charging occurs, as shown by the black line ('Battery current'), which peaks at +2.5 A. The orange line ('PV panel current') reflects solar current output, peaking at 7 A during high sun intensity and dropping to near zero in overcast conditions. Panel and battery voltages (blue and yellow lines) remain stable between 4.0–4.3 V, illustrating the energy balance and variability in solar input.

5.2. ANN Training for Panel Power Generation Prediction

Artificial intelligence models are trained using climatic data and measured values as output from the simulation model.

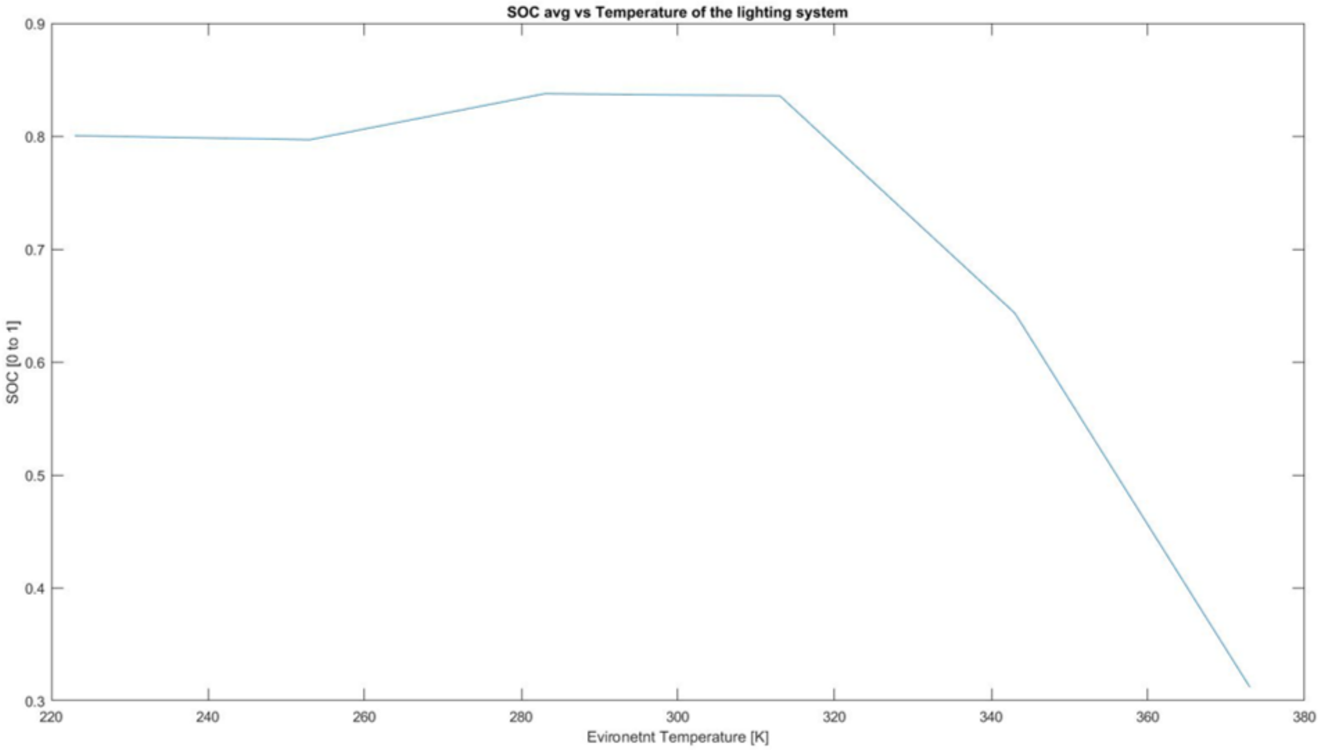

Figure 17.
AI predicted values and Simulink model data comparison, randomized solar radiation input data.

Figure 17 compares the predicted power values (in arbitrary units) from different machine learning models over the period from October 30 to November 5, 2024. The models include Linear Regression, GRU, LSTM, and Random Forest, alongside actual measured power values. Power fluctuations range from 30 to +35, with all models generally following the measured trends. LSTM provides the closest match to real data, while Linear Regression and GRU show larger local deviations. These results reflect the variability typical of solar generation and weather-dependent processes.

Random Forest regression, LSTM, Gated Recurrent Unit, and linear regression models were tested to predict SOC in the current work. The model was trained using output data generated by the Simulink model, with solar intensity and temperature as inputs.

The following table contains the resulting metrics for different AI models used for power prediction.

Table 1.
AI models' performance comparison.

Models	Test score	MSE	Test score train	MSE train
Lin Regression	2631	6923	2590	6707
LSTM	16408	269230	15671	245590
Rand Forest	2212	4894	1980	3919
GRU	5160	26627	4980	24798

Table 1 compares the performance of four power prediction models: Linear Regression, LSTM, Random Forest, and GRU. Random Forest yields the best results with a test score of 2.212 and a mean squared error (MSE) of 4.894. Linear Regression offers similar performance (score 2.631, MSE 6.923) but is less precise than the ensemble approach. LSTM and GRU exhibit higher error values (LSTM test MSE > 269,000; GRU ≈ 26,600), indicating overfitting or insufficient model tuning. These trends persist in training data, suggesting Random Forest and Linear Regression are the most effective for this task, while deep neural networks require further optimization.

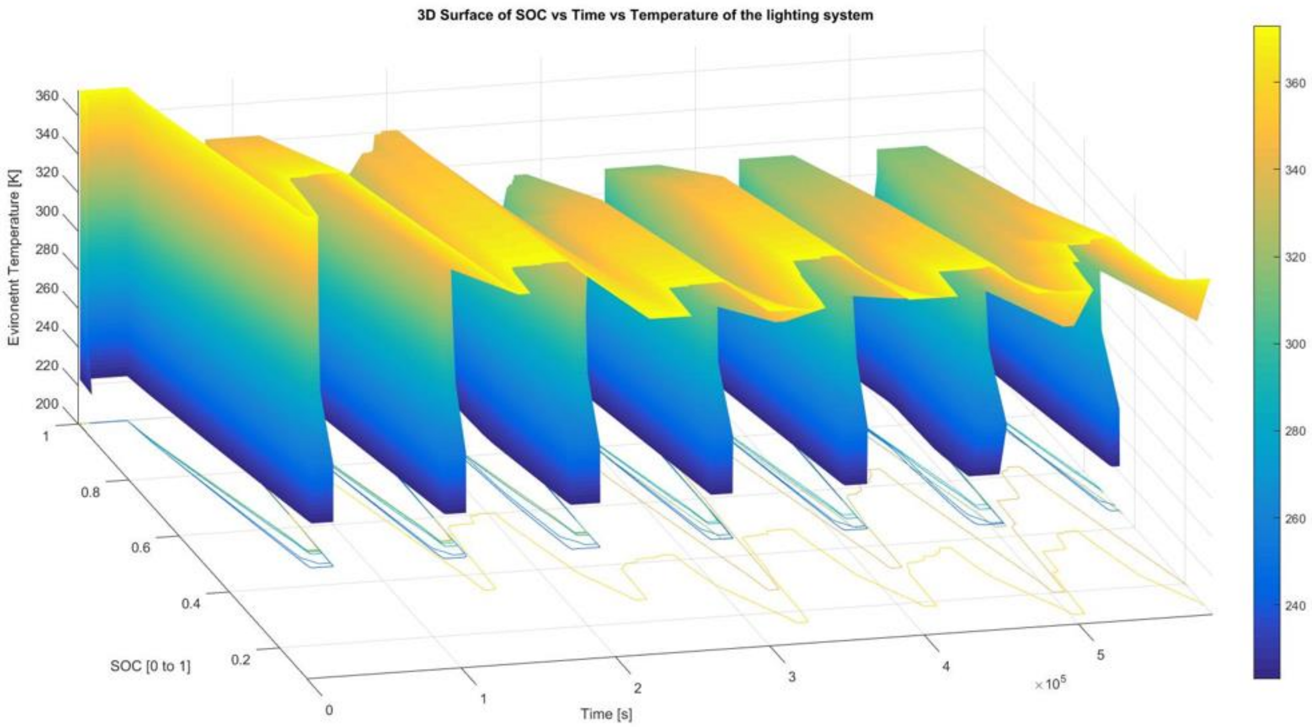

Figure 18.
Model output for the Almaty region.

Figure 18 shows the simulation model output for January in the Almaty region. On days with low solar irradiance, stored battery energy is fully depleted due to insufficient charging. During such periods, battery voltage drops below the threshold (e.g., 3.6 V), triggering an automatic switch to the external power source (see 'External Power' in Figure 13). The battery current drops to 0 A, and the LED lamp operates on grid power at night. After sufficient solar recharge, once the battery voltage exceeds 3.9 V, the system switches back to battery operation. This transition typically occurs after several overcast or snowy days.

6. Conclusion

This study developed a digital model of an intelligent solar-powered street lighting system implemented in MATLAB/Simulink and adapted to the conditions of Kazakhstan. Simulations showed that with a 200 W PV panel and 120 Ah battery, the system can autonomously operate LED lamps of up to 60 W for 72 hours, even under adverse weather conditions. Winter analysis indicated that the need for backup power increases to 27–32%, while in summer it remains below 8%. Applying AI models, particularly LSTM and GRU, achieved a mean SOC prediction error below 5%, enabling automated power switching and efficient energy distribution. The proposed architecture demonstrates strong potential for designing, testing, and deploying autonomous lighting systems in urban and rural areas of Central Asia. The model may serve as a tool for optimizing equipment parameters and intelligent lighting control under real climatic and operational constraints.

References

[1] United Nations Economic Commission for Europe, "Impact of artificial intelligence on the digital and data transformation in the electricity sector, committee on sustainable energy, Geneva, Switzerland," 2024. https://unece.org

[2] C. Subramani *et al.*, "Energy efficiency and pay-back calculation on street lighting systems," *AIP Conference Proceedings*, vol. 2112, no. 1, p. 020082, 2019. https://doi.org/10.1063/1.5112267

[3] A. Ożadowicz and J. Grela, "The street lighting integrated system case study, control scenarios, energy efficiency," in *Proceedings of the 2014 IEEE Emerging Technology and Factory Automation (ETFA), pp. 1-4. IEEE*, 2014.

[4] I. I. Maronchuk, I. B. Shirokov, A. A. Velchenko, and V. I. Mironchuk, "Intelligent LED lighting system," *ENERGETIKA. Proceedings of CIS Higher Education Institutions and Power Engineering Associations*, vol. 61, no. 5, pp. 440-450, 2018. https://doi.org/10.21122/1029-7448-2018-61-5-440-450

[5] I. Matveev, K. Karpov, I. Chmielewski, E. Siemens, and A. Yurchenko, "Fast object detection using dimensional based features for public street environments," *Smart Cities,* vol. 3, no. 1, pp. 93-111, 2020. https://doi.org/10.3390/smartcities3010006

[6] M. Abu Adma, S. Elmasry, M. Ahmed, and A. Ghitas, "Practical investigation for road lighting using renewable energy sources "Sizing and modelling of solar/wind hybrid system for road lighting application"," *Renewable Energy and Sustainable Development,* vol. 3, no. 3, pp. 258-266, 2017. http://dx.doi.org/10.21622/resd.2017.03.3.258

[7] D. Tukymbekov, A. Saymbetov, M. Nurgaliyev, N. Kuttybay, G. Dosymbetova, and Y. Svanbayev, "Intelligent autonomous street lighting system based on weather forecast using LSTM," *Energy,* vol. 231, p. 120902, 2021. https://doi.org/10.1016/j.energy.2021.120902

[8] N. Caroko and L. Kurniasari, "Solar energy utilization analysis on public street lighting in Sulur Kulon Progo," in *Proceedings of the International Conference on Technology, Community, and Environmental Development*, 2019.

[9] K. R. Valiullin, "Imitation modeling of the electrotechnical street lighting system," *Electrotechnical Systems and Complexes*, vol. 4, p. 41, 2018.

[10] G. Li, H. Wang, S. Zhang, J. Xin, and H. Liu, "Recurrent neural networks based photovoltaic power forecasting approach," *Energies*, vol. 12, no. 13, p. 2538, 2019. https://doi.org/10.3390/en12132538

[11] C. L. Dewangan, S. N. Singh, and S. Chakrabarti, "Combining forecasts of day-ahead solar power," *Energy*, vol. 202, p. 117743, 2020. https://doi.org/10.1016/j.energy.2020.117743

[12] M. Chai, F. Xia, S. Hao, D. Peng, C. Cui, and W. Liu, "PV power prediction based on LSTM with adaptive hyperparameter adjustment," *IEEE Access*, vol. 7, pp. 115473-115486, 2019. https://doi.org/10.1109/ACCESS.2019.2936597

[13] P. Nymann *et al.*, "Design, characterization and modelling of high efficient solar powered lighting systems," in *32nd European Photovoltaic Solar Energy Conference and Exhibition*, 2016.

[14] D. Akindipe, O. W. Olawale, and R. Bujko, "Techno-economic and social aspects of smart street lighting for small cities – a case study," *Sustainable Cities and Society*, vol. 84, p. 103989, 2022. https://doi.org/10.1016/j.scs.2022.103989

[15] Kaggle, "Solar power electricity production dataset. Kaggle," 2019. https://www.kaggle.com/datasets/ferhatmetin34/solar-power-electricity-production/data

[16] Joint Research Centre, "Photovoltaic geographical information system (PVGIS). PVGIS, European Commission," 2024. https://re.jrc.ec.europa.eu/pvg_tools/en/#TMY